ACS APPLIED MATERIALS & INTERFACES

Research Article

www.acsami.org

Novel Chemical Route to Prepare a New Polymer Blend Gate Dielectric for Flexible Low-Voltage Organic Thin-Film Transistor

Jagan Singh Meena,[†] Min-Ching Chu,[†] Yu-Cheng Chang,[†] Chung-Shu Wu,[†] Chih-Chia Cheng,[†] Feng-Chih Chang,[‡] and Fu-Hsiang Ko*[,†]

[†]Department of Materials Science and Engineering, and [‡]Department of Applied Chemistry, National Chiao Tung University, Hsinchu, Taiwan

Supporting Information

ABSTRACT: An organic−organic blend thin film has been synthesized through the solution deposition of a triblock copolymer (Pluronic P123, EO_{20}−PO_{70}−EO_{20}) and polystyrene (PS), which is called P123−PS for the blend film whose precursor solution was obtained with organic additives. In addition to having excellent insulating properties, these materials have satisfied other stringent requirements for an optimal flexible device: low-temperature fabrication, nontoxic, surface free of pinhole defect, compatibility with organic semiconductors, and mechanical flexibility. Atomic force microscope measurements revealed that the optimized P123−PS blend film was uniform, crack-free, and highly resistant to moisture absorption on polyimide (PI) substrate. The film was well-adhered to the flexible Au/Cr/PI substrate for device application as a stable insulator, which was likely due to the strong molecular assembly that includes both hydrophilic and hydrophobic effects from the high molecular weights. The contact angle measurements for the P123−PS surface indicated that the system had a good hydrophobic surface with a total surface free energy of approximately 19.6 mJ m^{-2}. The dielectric properties of P123−PS were characterized in a cross-linked metal−insulator−metal structured device on the PI substrate by leakage current, capacitance, and dielectric constant measurements. The P123−PS film showed an average low leakage current density value of approximately 10^{-10} A cm^{-2} at 5−10 MV cm^{-1} and large capacitance of 88.2 nF cm^{-2} at 1 MHz, and the calculated dielectric constant was 2.7. In addition, we demonstrated an organic thin-film transistor (OTFT) device on a flexible PI substrate using the P123−PS as the gate dielectric layer and pentacene as the channel layer. The OTFT showed good saturation mobility (0.16 cm^2 V^{-1} s^{-1}) and an on-to-off current ratio of 5×10^5. The OTFT should operate under bending conditions; therefore flexibility tests for two types of bending modes (tensile and compressive) were also performed successfully.

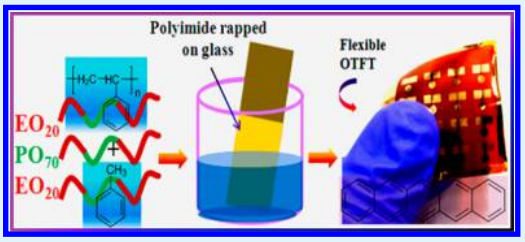

KEYWORDS: *flexible electronics, polymer gate dielectrics, polystyrene, pentacene, block copolymer, organic thin-film transistor*

1. INTRODUCTION

New organic-polymeric materials and devices have recently been the focus of research in the field of nanoelectrotechnology, primarily because of their resulting elastic properties compared to the properties of the individual constituents. These materials are widely pursued because they offer numerous advantages for developing flexible electronics, such as easy processing, low cost, low-temperature processing, and easily implemented structure modifications.[1,2] The use of various polymer materials as the dielectric layer in organic thin film transistors (OTFTs) has become a topic of interest, because they are produced using an inexpensive solution-phase process that is desirable for the planned commercialization of flexible OTFTs.[3] Polymer dielectrics are very attractive for electronics applications because they exhibit good characteristics that can often be obtained simply by spin-coating, casting, or printing under ambient conditions.[4,5] Organic and polymer materials have attracted considerable attention for the development of large-area, mechanically flexible electronic devices; therefore an inexpensive solution-phase processing method is desirable for the commercialization of OTFTs. These materials are widely pursued because they can be produced using many facile synthesis methods (e.g., spin-coating, dip-coating, printing, evaporation), they are highly compatible with a variety of substrates, including flexible substrates, and they present themselves the opportunity for structural modifications. Polymer materials with low dielectric constants (low-k) are known to decrease cross-talk noise and power dissipation, and when they are incorporated into device systems, they can dramatically decrease resistance-capacitance (R−C) delays. According to the International Roadmap for Semiconductors (ITRS) guidelines, intermetal insulating materials must have dielectric constants of approximately 2 to effectively obtain devices that are sized <100 nm.[6−8] There is currently a strong desire in the microelectronic industry to develop advanced, large-scale new composite polymer materials that can satisfy the growing demand for miniaturization with high-speed performance and flexibility. The goal is to develop an OTFT that has

Received: April 9, 2012
Accepted: June 5, 2012
Published: June 5, 2012

Scheme 1. Common Materials Used in This Work and a Schematic Representation of the Copolymer P123 and PS Precursors Mixed in Toluene and Chloroform, Which Were Employed for Fabricating the Polymer P123−PS Blend Thin-Film on a Flexible PI Substrate Using the Dip-Coating Process for Device Applications

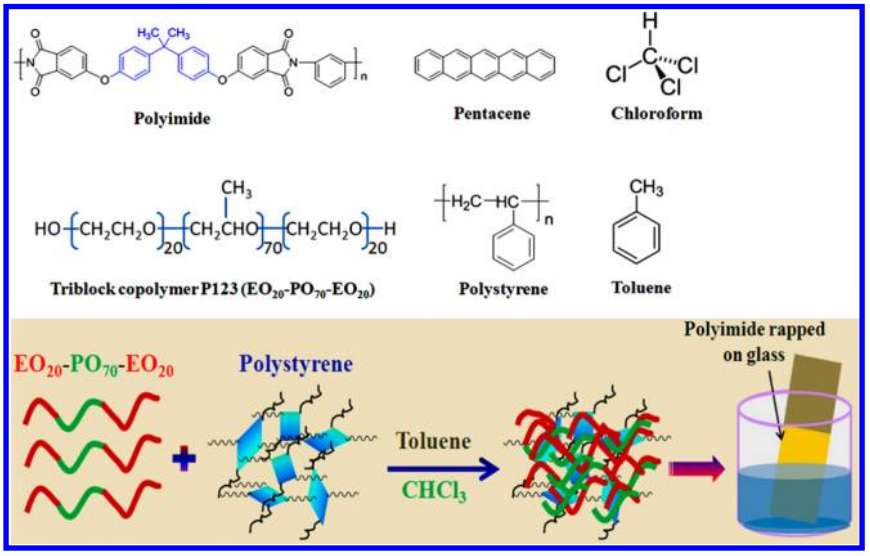

high mobility for certain semiconductor−polymer interfaces, which could be modulated to a very large extent. To be useful in technological applications, polymer films should have a morphology that either remains stable within an acceptable range of temperatures or undergoes a transformation that is controllable and predictable. However, searchers have had little success in developing new polymer low-*k* ultrathin films on flexible substrates at room temperature. Therefore, an investigation to determine the most suitable method for depositing the polymer thin films is needed; this method must consist of one or more distinct steps that can be performed at a low temperature.

In the field of organic and large area electronics, a major goal is the development of compatible materials sets, including semiconductors and insulators, which enable the fabrication of electronic circuits on flexible substrates at low cost and low temperature. The polymer blend dielectric strategy is a general approach to enhance the charge carrier mobility at low temperature.[9] There is a correlation between the semiconductor−polymer interface and the nature of the dielectric surface of chemical factors underlying such interfacial effects on a charge transport mechanism. The goal is to demonstrate that an OTFT with high mobility for certain semiconductor−polymer interfaces can be modulated to a very large extent. More recently, appropriate insulators that facilitate electron transport for typical organic p-type semiconductors have been used as active elements in optoelectronic devices such as organic light emitting diodes (OLED),[10] organic solar cells,[11] and OTFTs.[12] Organic semiconductors have many advantages, such as easy fabrication, mechanical flexibility, and low cost. Organic semiconductors offer the ability to fabricate an electronic device at a lower temperature and over a wide range of various substrates, such as plastic and paper. These materials can be processed using existing techniques that are employed in the semiconducting industry using chemical synthesis based dip-coating processing. This process for existing contributors can make drastic changes via low-cost, low-temperature processing and pervasive electronic applications such as flexible displays and radio frequency identification (RFID) tags.

In this study, we present for the first time an easy-to-follow chemical synthesis process for preparing new organic−organic P123−PS blend thin films for use as dielectric layers at low temperatures. This method provides a way to prevent the problem of pinhole defects in pure ultrathin polystyrene film. The electrical properties of the P123−PS blend thin film have been examined for advanced flexible metal-insulator-metal (MIM) capacitor applications. The electrical insulating properties of a flexible MIM device prepared using an organic−organic P123−PS blend thin film as a dielectric layer included low leakage current density and better capacitance density. In addition, the solution-processed blend films acted as a gate dielectric for the fabrication of pentacene OTFT devices on flexible polyimide (PI) substrate, making them suitable candidates for use in future flexible devices as a stable gate dielectrics. We also tested the functionality of our OTFT device under tensile and compressive bending modes without any deterioration and sterile loss in its electrical performance. These new polymer blend dielectric materials have good stability when they are used in electronic devices as composite dielectric layers and give excellent results compared to other polymer dielectric materials.

2. EXPERIMENTAL SECTION

2.1. Reagents and Materials. Pluronic P123 triblock copolymer, $HO(CH_2CH_2O)_{20}(CH_2CH(CH_3)O)_{70}(CH_2CH_2O)_{20}H$, (abbreviated P123 or $EO_{20}PO_{70}EO_{20}$, MW = 5800, BASF Corporation), is a difunctional block copolymer surfactant that is terminated with primary hydroxyl groups and a nonionic surfactant that is 100% active and relatively nontoxic. Polystyrene ($(C_8H_8)_n$, M_W = 54 000, Aldrich) or P123 was prepared in the solvents of chloroform ($CHCl_3$, 98%, Aldrich) and toluene ($C_6H_5CH_3$, Tedia Co. Inc.). Deionized water (DI water) was purified with filters and reverse osmosis, and deionized until the resistance was greater than 18 MΩ cm^{-1}. The DI water was used for cleaning, washing, and as a solvent. Chromium shots (Cr, 99.999%, Admat Inc.) 3−5 mm in size, aluminum shots (Al, 99.999%, Admat Inc.) 3−5 mm in size, and gold shots (Au, 99.999%, Admat Inc.) 1−2 mm in size, were purchased from Gredmann Taiwan Ltd. The organic semiconductor material pentacene ($C_{22}H_{14}$) was purchased from Seedchem Pty Ltd. (Electronic grade). DuPont Kapton Polyimide film, 38 μm in thickness and from the PV9100

series, was used as substrate to fabricate the device. All of the reagents were used without the further purification. Note that all of the experiments were performed in air or in a standard fume hood.

2.2. Preparation of the P123−PS Thin Film and Fabrication of the MIM and OTFT Devices. Scheme 1 presents the common synthesis method for preparing the P123−PS thin-film. In a typical synthesis experiment, polystyrene (4.5 g) was added to a mixture of P123 (1.5 g), toluene (15.2 mL), and chloroform (1.5 g) under static conditions. The reaction mixture is then stirred for 12 h using a magnetic stirrer at room temperature. After P123 and PS were completely dissolved in the toluene and chloroform, the solution was used to prepare the P123−PS composite thin film. The mixed solution was then applied by dip-coating onto a flexible PI substrate in two steps. First, the PI pasted onto glass substrate is immersed into the mixed solution for 5−10 s and then withdrawn. Second, the substrate was cured in a vacuum oven at 100 °C for 10 min. Then, further characterizations and applications in flexible electronic devices (MIM and OTFT) are investigated.

A DuPont Kapton plastic PI substrate with a thickness of 38 μm was used as the flexible substrate for fabricating the MIM capacitor and OTFT devices. The PI substrate was ultrasonically cleaned using ethanol (Fluka; water content: < 0.1%) for 30 min and then rinsed with DI water. A high-pressure stream of N_2 gas was then used to remove the water and any remaining particles from the PI surface. After being cleaned, the PI substrate was annealed at 200 °C for 1 h under vacuum to achieve relative thermal stability and to enhance the adhesion strength. Next, Cr (20 nm thick) and Au (80 nm thick) were sequentially deposited onto the PI substrate using a thermal coater. The Cr layer was used as the adhesion layer between the PI substrate and the Au thin film. Au was deposited as a gate electrode over the Cr layer on the PI substrate. Finally, the P123−PS film, which functioned as the dielectric layer, was deposited using the process described in the previous section, which consisted of immersing the sample strip into the solution and then curing it in a vacuum oven at 100 °C for 10 min. At the end of the experiments, Al films with a thickness of 300 nm were pattered as the top electrode using a shadow mask and a thermal coater. The electrical insulating properties of the P123−PS blend film have been optimized for OTFT on the PI substrate, which makes them suitable candidates for use as a stable intermetal dielectric in advanced flexible electronic devices. Cr and Au, which had thickness of 20 and 80 nm, respectively, were sequentially deposited through a shadow mask using a thermal coater to function as gate electrodes. Then, the P123−PS film was deposited using the solution dip-coating process as described in the previous section to function as an insulator layer. Pentacene film was then deposited as a channel layer using a thermal evaporator with the substrate temperature maintained at room temperature. Finally, source (S) and drain (D) Au electrodes with a thickness of 100 nm were deposited onto the pentacene/P123−PS/Au/Cr/PI through a shadow mask, which yielded the top-contact electrode OTFTs. The channel length (L) and width (W) were 70 and 1500 μm, respectively.

2.3. Thin-Film Characterizations and Electrical Measurements. The surface morphology of the blend film that coated the PI substrate was evaluated using atomic force microscopy (AFM, Digital Instruments Nanoscope, D−5000) with a scan size of 2 μm × 2 μm and a scan rate of 1 Hz. We used ellipsometery techniques to measure the thickness of the thin film. The FT−IR spectrum was recorded with the samples in KBr pellets (2 mg per 300 mg KBr) on an FT-IR spectrometer (model 580, Perkin-Elmer) with a resolution of 4.00 cm^{-1}. An infrared spectrum was recorded in the range of 500−4000 cm^{-1} to determine the functional groups in the molecular structure. The FT−IR measurement was performed at room temperature. The water contact angle on the film surface was measured using a commercial contact angle meter. Deionized water was used as the water source during the contact angle experiment. The contact angles were measured after the drop made contact with the film surface during testing of the flexible PI substrate. The XRD pattern for the organic pentacene film was recorded using a Rigaku D/max−IIIB diffractometer with Cu K_α radiation (λ = 1.5406 Å). The leakage currents and capacitances in the MIM structured device with the blend film were measured using an Agilent−4156 probe station and an HP−4284A capacitance−voltage analyzer, respectively. The output and transfer characteristics of the OTFT were measured using an Agilent−4156 probe station under ambient conditions.

We examined two additional properties of our OTFT on the PI substrate to explore its feasibility for use in practical applications. We estimated the mechanical strain on the electrical properties during the flexibility test, which includes tensile and compressive strains for minimum radii of curvature (R_c =1.5 cm). Before the manufacturing process, a piece of foil was used as a support substrate to provide the specific bending conditions for the convex and concave settings for a radii of curvature of 1.5 cm, (shown elsewhere in this text). We also calculated the maximum strain at which the OTFT device can be bent to a radius of curvature of 1.5 cm without any degradation loss.

3. RESULTS AND DISCUSSION

3.1. P123−PS film Surface Roughness and FT−IR Analysis. When a new cross-linked polymeric dielectric film is fabricated on a flexible substrate, it is necessary to optimize the nature of the film surface. AFM data provide important information about the surface roughness for initial material evaluation. It is well-known that pure PS films with a thickness less than 100 nm suffer from pinhole defects, as reported previously.[13−15] In our experiment, we also observed the pinhole defects in the polystyrene film with a thickness of approximately 20 nm, as shown in Figure S1 in the Supporting Information. However, this problem was prevented when we used P123 and PS mixed with organic additives, and the P123−PS blend film was successfully deposited without any pinhole defects. The thickness of the film was 28 nm, as estimated using ellipsometery techniques. The surface morphology of the P123−PS film was investigated using AFM with a scan size of 2 μm × 2 μm, as shown in Figure 1a. For the AFM image, the sample was prepared using a dip-coating process onto a flexible PI substrate. The surface morphology of the P123−PS film

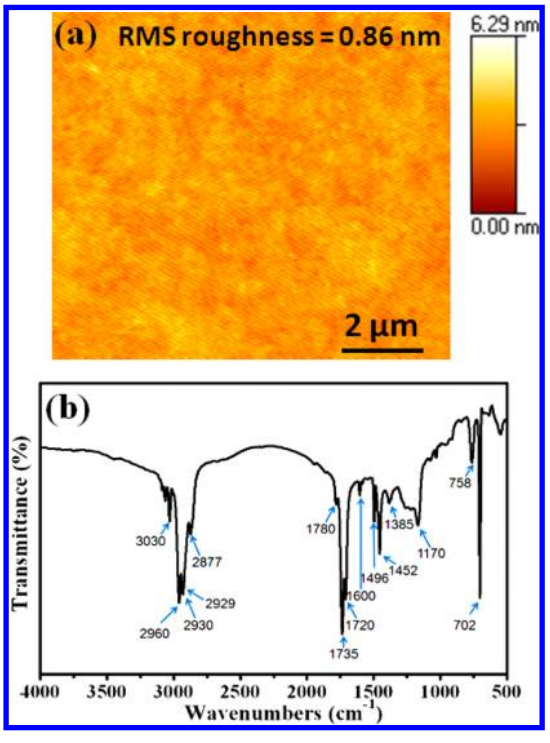

Figure 1. (a) AFM image and (b) FT−IR spectrum of the P123−PS thin film (cured at 100 °C) coated onto a flexible PI substrate.

deposited onto the flexible PI is uniform, and a crack-free surface has been produced, which is clearly observed in the image. The average root-mean square (R_{rms}) roughness evaluated from the P123−PS AFM image was approximately 0.86 nm. In the case, the possible reason for the better surface roughness in P123−PS may be the presence of P123. It is believed that during the in situ deposition of the matrix composite, P123 functions as a uniform structure-directing agent.[16] In a ternary system, the P123 block copolymer facilitates the deposition of a uniform film through organic−organic cooperative assembly. It is well know that, in a ternary copolymer-selective solvent system, block copolymers can self-assemble into a variety of lyotropic liquid crystals micro-structures that consist of lamellar, cubic or hexagonal structures.[16,17] After analyzing the surface morphology of the polymer blend film, we confirmed that the deposited P123−PS film was crack-free, uniform, and well-adhered to the surface of the PI substrate.

From a physical perspective, the major differences arise from the rather weak intermolecular forces that bind the molecules together in π−conjugated organic solid and the chains in polymer compounds. The addition of pluronic P123 resulted in an association of the surfactant molecules with the PS micelles and mixed micelles are formed. The size and structure of the mixed micelles and the interparticle interactions were studied by varying the surfactant-to-copolymer (P123/PS) molar ratio. The novelty of this study lies in the composition-induced structural change of the mixed micelles with aging at constant temperature. The current mechanism is only a theoretical assumption and is not confirmed by any experimental analyses. When the solution is used to deposit the film, the film gradually changes to a stable polymer-blend film during in situ growth, and is self-organized for further characterizations and device applications.

To gain more insight about the functional groups, FT−IR spectroscopy was used to examine the functional groups of the polymer blend P123−PS thin film surface. The IR absorption spectrum of the organic P123−PS blend thin film after calcining at 100 °C is presented in Figure 1b. The spectra for the P123−PS films that were deposited with an organic additive thin film have a sharper spectral profile, which indicates that these films have a less disordered structure. As shown in Figure 1b, a sharp peak resulting from the benzene functionalized PS stretching mode appears at 720, 758, 1385, and 1452 cm^{-1} in the absorption spectrum. The two peaks at 2929 and 3030 cm^{-1} are due to the methylene group in PS. The bands between 2877 and 2960 cm^{-1} are believed to be due to CH_3, CH_2, and CH stretching, which can be detected from the P123 copolymer, whereas the sharp peak at 1170 cm^{-1} for the C−O−C bending mode likely resulted from the P123. It is difficult to determine the origin of the 1720, 1735, and 1780 cm^{-1} peaks, which appeared from C═O group of the organic PI surface. The peaks at 1496 and 1600 cm^{-1}, which resulted from stretching mode of the C═C in the ring for PS or the PI surface, can also be detected. The IR spectrum of our P123−PS blend thin film coating the PI substrate is more consistent for PS and P123 separately over silicon for the functional group, which reported previously.[18,19] From the FT−IR spectrum, it could be concluded that toluene and chloroform were successfully removed when the sample was calcined at 100 °C. Finally, we concluded from the results that the sample consisted of PS, P123, and a trace amount of contaminating carbon; no other impurities (e.g., chloride and organic ions) were present on the film surface. Moreover, The IR absorption spectrum of the organic P123−PS blend thin film without any curing process is also depicted in Figure S2 in the Supporting Information The spectrum for the P123−PS film deposited with an organic additive thin film did not show a sharper spectral profile such as observed for the P123−PS film that was cured at 100 °C. Therefore, it could be expected that the P123−PS film without temperature curing has a disordered structure due to the presence of organic impurities.

3.2. Contact Angle and Surface Energy Measurements of the P123−PS Film. We combine an experimental and theoretical study to characterize the aggregation steps at the surface of the P123−PS blend film. This blend surface produced using the P123 copolymer and PS is of great interest in its own right. DI water, ethylene glycol and diiodomethane contact angle measurements were conducted to investigate the surface free energy of the P123−PS blend surface. The contact angle of a sessile drop on the P123−PS layer was directly measured by aligning a tangent for 5−10 min with the drop profile at the point of contact with the surface. The total surface energy is another quantifiable characteristic that affects pattern formation, from which the detailed energy contributions from the polymeric polar and apolar terms can be individually extracted.[20] The surface tension (γ_i) of phase i can be expressed as

$$\gamma_i = \gamma_i^{LW} + \gamma_i^{AB} = \gamma_i^{LW} + 2\sqrt{\gamma_i^{+}\gamma_i^{-}} \quad (1)$$

where γ_i^{LW} and γ_i^{AB} represent the dispersion (apolar) and polar terms of the surface tension, respectively, and γ_i^{+} and γ_i^{-} are the electron acceptor and electron donor parameters, respectively, for the polar component. The following contact angle equilibrium, based on the Young−Dupre equation, was formulated by Van Oss et al.[21] to describe the interfacial tension between the liquid (L) and the polymer surface (S)

$$(1 + \cos\theta_c)\gamma_L = 2\left(\sqrt{\gamma_S^{LW}\gamma_L^{LW}} + \sqrt{\gamma_S^{+}\gamma_L^{-}} + \sqrt{\gamma_S^{-}\gamma_L^{+}}\right) \quad (2)$$

where θ_c is the contact angle determined using three different liquids with known values of γ_L^{LW}, γ_L^{+}, and γ_L^{-}; e.g., water (21.8, 25.5, and 25.5 mJ m^{-2}, respectively), ethylene glycol (29, 1.92, and 47 mJ m^{-2}, respectively), and diiodomethane (50.8, 0, and 0 mJ m^{-2}, respectively). A three-liquid procedure was proposed to measure the surface tension and its three components of any solid surface. The contact angles of water, ethylene glycol and diiodomethane were measured immediately following the treatment. For the P123−PS polymer blend film, the contact angles of water, ethylene glycol, and diiodomethane were 92, 98, and 86°, respectively, and are shown in Figure 2a. A schematic representation of the surface tension of P123−PS surface over PI is depicted in Figure 2b. Thus, the calculated values of the surface tensions γ_S, γ_S^{LW}, γ_S^{+}, and γ_S^{-} for the P123−PS film were 19.6, 14.5, 0.39, and 16.4 mJ m^{-2}, respectively. The total surface energy for P123−PS is comparable to the total surface energy for a pure PS surface, i.e., 19.13 mJ m^{-2}.[22] The improvement of the stable hydrophobic surface due to the incorporation of P123 is the main reason for the suppression of the lowest surface energy in the blend surface.

A possible mechanism for the formation of the hydrophobic surface from the aggregation of P123 and PS into the organic additive is shown in Figure 2c. The hydrophobic assembly nature of P123-PS suggests that this new polymer blend film could potentially be used for screening excellent hydrophobic

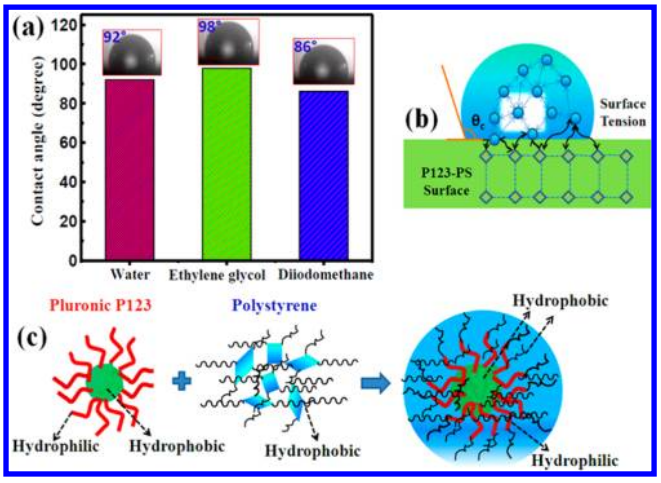

Figure 2. (a) Contact angle measurements for water, ethylene glycol and diiodomethane with the drop images at the point of contact on the P123–PS surface; (b) schematic representation of surface tension of P123–PS surface over PI; (c) possible mechanism for the formation of a hydrophobic surface from the aggregation of P123 and PS into the organic additive.

surface mutants and for isolating of hydrophobic bacteria from nature. In addition, in OTFTs, the surface of the dielectric layer is important for effective performance because it allows for a conducting channel in the interface between the dielectric layer and the semiconductors. The surface energy of the dielectric layer enables the vertical growth of pentacene molecules, and the holes could easily be moved in the vertical direction of the pentacene molecules; these vertical pentacene alignments enhance mobility in OTFTs.[23]

3.3. Electrical Measurements of the MIM Capacitor Device. A capacitor (formerly known as condenser) is a passive two-terminal electrical component used to store energy in an electric field. The forms of practical capacitors vary widely, but all contain at least two electrical conductors that are separated by a dielectric (insulator). When there is a potential difference (voltage) across the conductors, a static electric field develops across the dielectric, thereby causing a positive charge to collect on one plate and a negative charge on the other plate. In practice, the dielectric between the plates passes a small amount of leakage current and has an electric field strength limit, resulting in a breakdown field. Electrical characterizations were performed to investigate the electrical insulation properties of the polymer blend film. Leakage current density-electric field (J–E) measurements were performed on the P123–PS blend thin film in a MIM structured device, as shown Figure 3a and the sample-image in Figure 3b to determine the leakage current characteristics and dielectric breakdown field. The J–E response is also used to determine the available range for high-quality capacitance density–voltage (C–V) measurements. First, we measured the insulator properties for the PS film, as shown in Figure S3 in the Supporting Information. Note that the device performance was poor because the leakage current was very high ($\sim 1 \times 10^{-4}$ A cm^{-2}) and the breakdown field was very low (<1 MV cm^{-1}) because the film was affected by pinhole defects. However, the insulating properties were enhanced for the P123–PS film because this film was free of pinhole defects. Panels c and d in Figure 3 show typical J–E and C–V plots for the MIM configurations fabricated using the P123–PS blend thin-film as an insulator layer. As observed in Figure 3c, the average low leakage current density value of the P123–PS film was estimated to be approximately 1×10^{-10} A cm^{-2} at an applied electric field between 5–10 MV cm^{-1}. The probe was moved to three different points in a random order on the P123–PS based MIM capacitor and exhibited leakage current values that were higher or lower than the average leakage current value and a good breakdown limit of the film. We examined the leakage current at three different points to

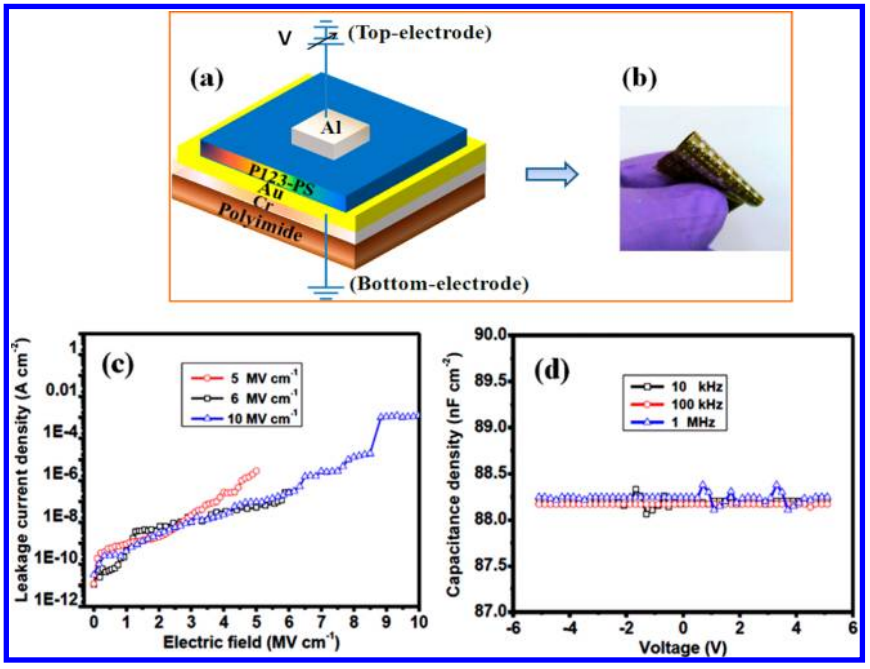

Figure 3. (a) Schematic view of the P123–PS blend thin film-based MIM capacitor; (b) photograph of a flexible MIM capacitors on area of 5 × 5 cm^2 on flexible PI substrate showing the sample bent by hand; (c) J–E and (d) C–V plots for MIM structured device fabricated using the P123–PS blend thin film as a gate insulator layer.

Table 1. Comparison of the Electrical Properties of Various Low-*k* Dielectric Materials[a]

ref	material	film thickness (nm)	rms roughness (nm)	dielectric constant	leakage current density (A cm^{-2})	substrate
this work	P123–PS	28	0.86	2.7	$\sim 1 \times 10^{-10}$	polyimide
24	PMMA	100	0.52	3.5	$\sim 1 \times 10^{-7}$	glass
25	PVP	133	6	6.4	$\sim 1 \times 10^{-8}$	silicon
25	PS	122	2	2.6	$\sim 1 \times 10^{-9}$	silicon
25	CPVP–C_n	18–20	2–8	6.1–6.5	1×10^{-9} to 1×10^{-10}	silicon
25	CPS–C_n	10–13	1–10	2.5–3.0	1×10^{-8} to 1×10^{-9}	silicon
4	PAA	330	4	4.9	$\sim 1 \times 10^{-8}$	ITO glass
25	SiO_2	300	2	3.9	1×10^{-9} to 1×10^{-10}	silicon
26	Al_2O_3	120		8.6	1×10^{-8} to 1×10^{-9}	silicon

[a] n = 0, 2, 6, and a = calculated dielectric constant.

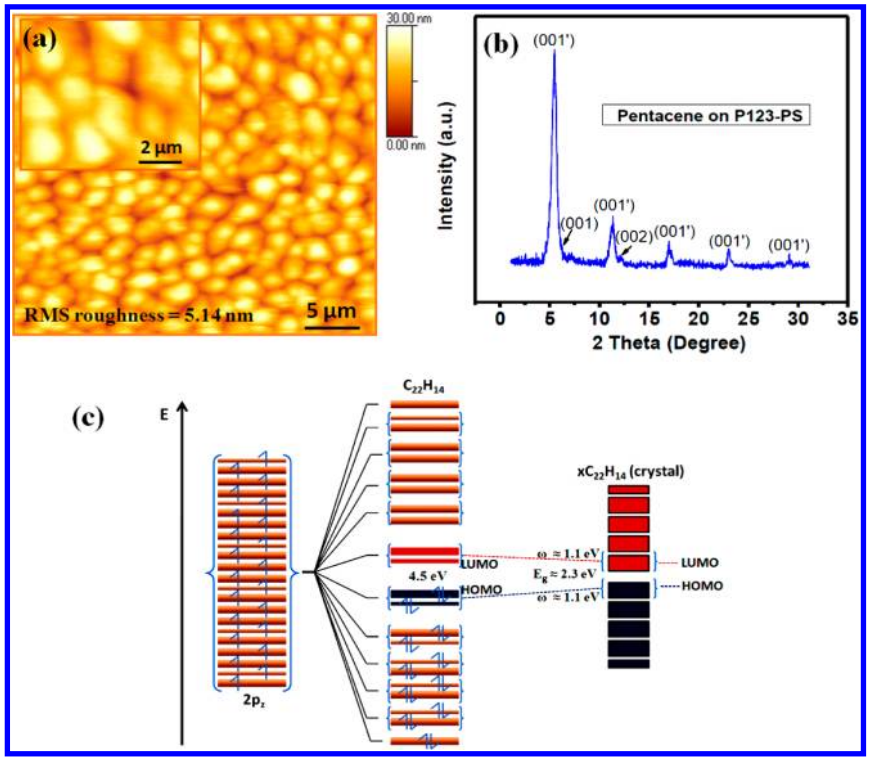

Figure 4. (a) AFM image, (b) XRD pattern from the pentacene film deposited on the P123–PS film over Au/Cr/PI substrate, and (c) schematic representations of the orbital energies and the corresponding symmetries of the molecular orbitals of a pentacene molecule in the HOMO–LUMO states obtained from density-functional theory calculations.

determine the breakdown limit and the insulating quality of our film. The breakdown field for the P123–PS blend film was approximately 8.5 MV cm^{-1}. On the basis of this result, we concluded that the film is of very high quality and exhibited extremely good insulating properties.

Figure 3d displays a characteristic *C*–*V* plot for P123–PS. As shown in Figure 3d, the capacitance of the P123–PS blend film atthree different frequencies of 10 kHz, 100 kHz and 1 MHz are 88.12, 88.18, and 88.24 nF cm^{-2}, respectively. The *J*–*E* and *C*–*V* results demonstrated that the blend film generated using P123 and PS dissolved in organic solvents exhibit superior insulating properties compared to the corresponding neat polymers and many other previously reported materials (Table 1).[4,24–26]

Furthermore, according to the capacitance and thickness data, we evaluated the *k*–value of the P123–PS blend film using the following equation[27]

$$C_{\mathrm{P123-PS}} = \frac{C}{A} = \frac{k\varepsilon_0}{d} \tag{3}$$

where k is the dielectric constant of insulator, $\varepsilon_0 \approx 8.85 \times 10^{-12}$ F m^{-1} and is the permittivity of vacuum, A is the area of the capacitor, and d is the thickness of the insulator layer. The average *k*–value of the P123–PS film is approximately 2.7, which was estimated from the average value of three point measurements for $C_{\mathrm{P123-PS}}$ that was approximately 88.2 nF cm^{-2}. This calculated low-*k* value is consistent with other polymer gate dielectrics, which are listed in Table 1. The obtained results indicate that the P123–PS blend polymer is a good potential candidate to replace SiO_2 or other low-*k* intermetal dielectric materials and that it could be an ideal alternative for flexible devices. Furthermore, flexible capacitors developed using this blend polymer could be widely used in electronic circuits for blocking direct current while allowing alternating current to pass, such as in filter networks to smooth the output of power supplies in resonant circuits that tune

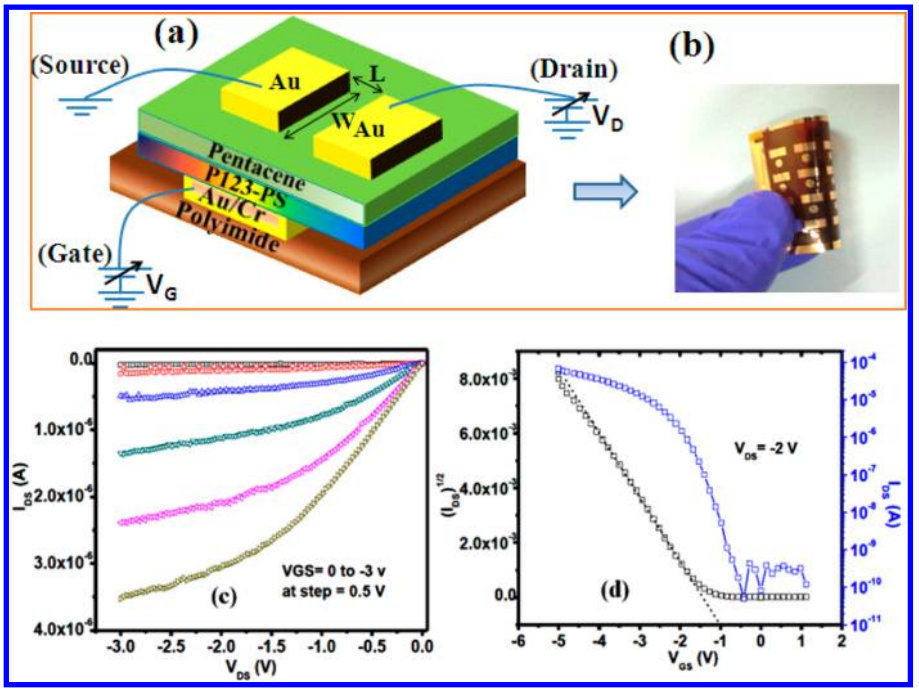

Figure 5. (a) Schematic representation of the OTFT device that features P123−PS as a gate insulator and pentacene as a semiconductor layer; (b) photograph of the OTFT devices on a 5 × 5 cm^2 area on flexible PI substrate and plots for the OTFT; (c) output characteristic (I_{DS}−V_{DS}), where V_{GS} ranges from 0 to −5.0 at −1 V step, and (d) transfer characteristic (I_{DS}−V_{GS}), when V_{DS}= −2 V.

radios to particular frequencies and in many other applications. These blend film-based capacitors have been proposed to be excellent general-purpose plastic film capacitors, which are ideal for low-power RF and precision analog applications.

3.4. Pentacene: Model for Ordered Organic Semiconductors. The high-quality interface between an insulator and semiconductor layers dramatically impacts semiconductor devices for practical applications with respect to their operation and use in the electric power industry. It has been suggested that higher mobilities may be achieved by designing π−conjugated molecules that stack face-to-face (π−stacking) in the close crystalline state, thereby increasing the intermolecular interactions.[28,29] Therefore, we used the typical crystal structured planar π-conjugated pentacene for the semiconductor organic layer to develop the OTFT device using the P123−PS blend polymer as a gate insulator. Panels a and b in Figure 4 show the AFM image and reflective XRD pattern of a 50-nm-thick pentacene layer grown over P123−PS/Au/Cr/PI substrate. The AFM and XRD experiments were performed to investigate the effects of the surface properties of pentacene on the surface morphology of the P123−PS blend film. The AFM image of pentacene at a scale length of 5 μm (Inset: 2 μm) demonstrated the crystalline quality (Figure 4 a). The R_{rms} evaluated from the AFM image of pentacene is 5.14 nm. The AFM images of the pentacene layer over the P123−PS surface revealed the growth of a thick, uniform, high-quality film. The data suggest robust and almost symmetric crystalline pentacene that also has large, densely packed, and well-interconnected grains. The growth morphology of pentacene was similar to those prepared on silicon and PI substrates as previously reported.[30,31]

The structure of the pentacene layer was elucidated from the XRD data (Figure 4b) collected in reflection mode at 20 kV with Cu $K\alpha$ radiation (λ = 1.5406 Å) with a coupled (θ−2θ) scans configuration. The corresponding XRD pattern contains a series of sharp (0 0 k) peaks, which indicates that the pentacene film is highly ordered. The first peak at 5.3° (thin-film phase) corresponds to a lattice parameter of 15.6 Å. The XRD analysis indicated that the pentacene films on P123−PS have a better crystalline quality. The crystallite size was estimated from the broadening of the diffraction peaks using the Scherrer equation: $D = 0.89\lambda/\beta \cos\theta$, where D is the crystallite size, λ is the wavelength of the x−ray radiation (λ = 1.5406 Å), β is the peak width at half-maximum height after subtraction of the equipment broadening, 2θ = 5.3° for (101), and 0.89 is the Scherrer constant. The estimated grain size for the pentacene film based on the Scherrer formula applied to the broad peak at 5.3° is approximately 500 nm.

Pentacene is the material of choice for research on OTFTs because of its good charge carrier mobility and its ability to form a large, well-ordered crystalline structure. Pentacene exhibits a conjugated π-electron system, which is formed from the p_z orbitals of sp^2-hybridized atoms that extends over the entire molecule. In a single pentacene molecule, the weakest π-bonding results in a lower electronic excitation (π−π* transitions). The occupied π level is also commonly called highest occupied molecular orbital (HOMO), whereas the unoccupied π* level is referred to as lowest unoccupied molecular orbital (LUMO). As in inorganic solid materials, the electron levels responsible for the electrical conduction are the ones that are closest to the Fermi level, which lies between the HOMO and the LUMO and therefore characterize the electronic states responsible for the conduction and the optical properties. The band structures of the conjugated pentacene molecules are schematically represented in Figure 4c. The larger molecular orbitals (HOMO−LUMO) become narrow bands (small bandwidth, $\omega \approx 1.1$ eV) and result in for better π−π* overlap to reduce the energy bandgap by approximately 2.3 eV.

In general, the HOMO−LUMO gap in pentacene is found to be 2.7 eV. Therefore, assuming a relative molecular orientation similar to the single-crystal phase, both of the HOMO and LUMO bandwidths increase by a few tenths of an electron volt with respect to the bulk phase, with a consequent reduction in the energy band gap. This theoretical explanation suggests that the assumed molecular arrangement is a possible candidate for the orientation in real pentacene thin film sample, and calls for further experimental work aimed at determining the real mutual molecular orientation. This theoretical simulation for the pentacene molecule is based on the excellent agreement with a recent study,[32] as far as the symmetries and the orbital character of HOMO and LUMO are concerned. Therefore, the strong contribution of the $2p_z$ orbitals in the HOMO and LUMO of pentacene is the molecular reason for the semiconductivity behavior of pentacene. Compared to inorganic crystals, the reduced bandwidth tends to localize the charges. However, in the case of single crystalline pentacene, the valence and the conduction bands are replaced by the HOMOs and LUMOs of the organic crystals, which are mainly located at the molecules sites but weakly interact with each other. Only at low temperatures and in the case of pentacene with well-ordered, purified organic crystals can the transport be described in terms of band transport. Therefore, in our experiment, pentacene is a better semiconductor active channel layer choice than other organic materials in the development of the OTFT.

3.5. Electrical Measurements from the OTFT Device. To demonstrate the performance of the polymeric P123−PS blend film as a dielectric layer, we fabricated a pentacene-based OTFT with the device geometry shown in Figure 5a; a sample image is shown in Figure 5b. Figure 5c represents the drain current-drain voltage (I_{DS}−V_{DS}) output curve obtained from our OTFT that use P123−PS as a dielectric layer and pentacene as channel layer with a length (L) = 70 μm and a channel width (W)= 1500 μm. The device demonstrated desirable low-operating voltage p-type OTFT characteristics at an operating voltage of −5 V. The maximum saturation current of $\sim 6.1 \times 10^{-5}$ A was achieved at V_{GS} = −5 V. The observed OTFT characteristics both closely conformed to conventional transistor characteristics in the linear and saturation regimes to the drain current that increased linearly at low drain voltage and demonstraed clear saturation behavior at high drain voltage. The drain current-gate voltage (I_{DS}−V_{GS}) transfer curve of pentacene OTFT on P123−PS blend gate dielectrics (Figure 5d) indicated that the OTFT yielded high current on/off ratios ($I_{on/off} = 5 \times 10^5$) and negligible gate-sweep hysteresis. The carrier mobility, (μ_{OTFT}) and threshold voltage (V_{th}) values were calculated in the saturation regime using the following equation[33,34]

$$I_{DS} = \mu_{OTFT} C_i \frac{W}{2L} (V_{GS} - V_{th})^2 \quad (4)$$

where, C_i is capacitance of the polymer blend P123−PS gate dielectric. The OTFT displayed a V_{th} of approximately −1 V and a carrier mobility of 0.16 $cm^2\ V^{-1}\ s^{-1}$. The OTFT performance is comparable to values recently reported for polymer gate dielectrics and surpasses those of devices employing organic semiconductor materials for the channel layer grown on a silicon/glass substrate.[35,36] Therefore, replacement of the traditional gate dielectrics used in complementary metal-oxide semiconductor (CMOS)-like logic circuits with the polymer blend gate dielectric systems introduced here requires the formation of an OTFT at the interface between the organic semiconductors and the P123−PS gate dielectric.

3.6. Flexibility Test and Strain-Estimation for OTFT. Every material, in its native form, has an inherent molecular structure that leads to certain behaviors in terms of film stress. Therefore, to determine the feasibility of our OTFT device, we examined two additional features for its use in practical applications. Namely, we estimated the transfer characteristics both in the tensile mode (see Figure S4a in the Supporting Information) and the compressive mode (see Figure S4b in the Supporting Information) for a minimum radius of curvature (R_c) of 1.5 cm to determine the maximum strain for our OTFT. Before the manufacturing process, a hard plastic foil was used as a substrate support to establish these specific bending conditions presented in the inset of Figure S4 in the Supporting Information. The transfer characteristics reveal some changes in terms of the on-to-off current (3×10^5), V_{th} (− 0.8 V), and mobility (~0.15 $cm^2\ V^{-1}\ s^{-1}$) when both tensile and compressive strains were applied. The effects of bending strain on the structure and electrical characteristics of the pentacene films in flexible devices were investigated. These bending-stress-driven phase transitions between the bulk phase and the thin-film phase in the pentacene film resulted minor changes in field-effect mobility of our pentacene based flexible OTFT. The results from our study were also in agreement with effects of bending strain on the mobility of pentacene films in flexible devices that resulted in changes in the field-effect mobility in the previous study.[37] We concluded from the results that a flexible OTFT device with good transistor properties has been developed using P123−PS as a gate insulator and pentacene as a p-channel organic semiconductor. Additionally, we deduced that mechanical strains influence the energy barrier height between the grains of the pentacene thin films, thereby resulting in the variation of the channel resistances. Finally, the fatigue test revealed that our flexible OTFTs in this study exhibited supreme flexibility, especially under tensile and compressive bending conditions for a minimum radius of curvature of approximately 1.5 cm. The flexible PI substrate is bent into convex and concave shapes, where the outer surface experiences tensile strain and the inner surface compressive strain, as indicated in Figure S5 in the Supporting Information and calculated using simple approximations for the film strain and radius of curvature.

4. SUMMARY

In summary, we developed an innovative approach for the deposition of a new organic−organic (P123−PS) blend thin film on a flexible polyimide substrate using a novel chemical dip-coating method at low temperature. The planar aggregation of pluronic EO_{20}−PO_{70}−EO_{20} triblock copolymer P123 and polystyrene materials is likely due to the strong assembly of hydrophobic and hydrophilic molecular interactions and high molecular weights. Because of the good insulating properties of our polymer blend film, it could be an ideal dielectric film for use in future in device applications. The time-induced contact angle measurement using water, ethylene glycol and diiodomethane for P123−PS revealed a good hydrophobic surface with a total surface free energy of 19.6 mJ m^{-2}. In addition, the polymeric P123−PS in a sandwich-like configuration (e.g., metal−insulator−metal) exhibits a low leakage current density value ($\sim 1 \times 10^{-10}$ A cm^{-2}) and good capacitance density (88.2 nF cm^{-2}). An OTFT device employing P123−PS as a gate

insulator and the conjugated π-electron system organic pentacene as a semiconductor layer was successfully constructed and exhibited excellent device performance (e.g., carrier mobility, 0.16 $cm^2 V^{-1} s^{-1}$; on-to-off current ratio, 5×10^5) and good device stability. Furthermore, the performance of the OTFT device under bending modes of tensile and compressive strain are among the best results for these materials, which adopt a bottom-gate configuration; these results are attributed to the high-quality dielectric-organic semiconductor interface that was formed. Finally, it should be emphasized that this novel solution processed dip-coating method provides a new way to investigate the surface of polymeric blend films and could be a promising approach for practical applications because it is a low-cost and low-temperature manufacturing technique.

■ ASSOCIATED CONTENT

Ⓢ Supporting Information

A detailed AFM image, leakage current density measurements for the PS film, FT−IR results for uncured blend film, and flexibility tests. This material is available free of charge via the Internet at http://pubs.acs.org/.

■ AUTHOR INFORMATION

Corresponding Author

*E-mail: fhko@mail.nctu.edu.tw. Tel.: +886-35712121-55803. Fax: +886-35744689.

Notes

The authors declare no competing financial interest.

■ ACKNOWLEDGMENTS

The authors thank the National Device Laboratories (NDL) for their support in device fabrication and the National Science Council of the Republic of China, Taiwan, for financially supporting this research under Contracts 99-2120-M-009-008 and NSC 98-2113-M-009-017.

■ REFERENCES

(1) Sekitani, T.; Zschieschang, U.; Klauk, H.; Someya, T. *Nat. Mater.* **2010**, *9*, 1015−1022.
(2) Yang, H.; Yang, C.; Kim, S. H.; Jang, M.; Park, C. E. *ACS Appl. Mater. Interfaces* **2010**, *2*, 391−396.
(3) Li, L.; Hu, W.; Chi, L.; Fuchs, H. *J. Phys. Chem. B* **2010**, *114*, 5315−5319.
(4) Lim, S. H.; Kim, J.; Lee, S.-G.; Kim, Y. S. *Chem. Commun.* **2010**, *46*, 3961−3963.
(5) Kim, B. S. H.; Hong, K.; Jang, M.; Jang, J.; Anthony, J. E.; Yang, H.; Park, C. E. *Adv. Mater.* **2010**, *22*, 4809−4813.
(6) Shamiryan, D.; Abell, T.; Iacopi, F.; Maex, K. *Mater. Today* **2004**, *7*, 34−39.
(7) *The International Technology Roadmap for Semiconductors*; Semiconductor Industry Association, SEMATECH: Austin, TX, 2007.
(8) Volksen, W.; Miller, R. D.; Dubois, G. *Chem. Rev.* **2010**, *110*, 56−110.
(9) Yoon, M.-H.; Kim, C.; Facchetti, A.; Marks, T. J. *J. Am. Chem. Soc.* **2006**, *128*, 12851−12869.
(10) Zhong, C.; Duan, C.; Huang, F.; Wu, H.; Cao, Y. *Chem. Mater.* **2011**, *23*, 326−340.
(11) Hoth, C. N.; Schilinsky, P.; Choulis, S. A.; Brabec, C. J. *Nano Lett.* **2008**, *8*, 2806−2813.
(12) Ha, Y.-G.; Jeong, S.; Wu, J.; Kim, M.-G.; Dravid, V. P.; Facchetti, A.; Marks, T. J. *J. Am. Chem. Soc.* **2010**, *132*, 17426−17434.
(13) Bai, J.; Snively, C. M.; Delgass, W. N.; Lauterbach, J. *Macromolecules* **2001**, *34*, 1214−1220.
(14) Ma, M.; He, Z.; Yang, J.; Chen, F.; Wang, K.; Zhang, Q.; Deng, H.; Fu, Q. *Langmuir* **2011**, *27*, 13072−13081.
(15) Reiter, G. *Langmuir* **1993**, *9*, 1344−1351.
(16) Tiwari, J. N.; Meena, J. S.; Wu, C.-S.; Tiwari, R. N.; Chu, M.-C.; Chang, F.-C.; Ko, F.-H. *ChemSusChem* **2010**, *3*, 1051−1056.
(17) Foster, B.; Cosgrov, T.; Hammouda, B. *Langmuir* **2009**, *25*, 6760−6766.
(18) Shen, B.; Zhai, W.; Chen, C.; Lu, D.; Wang, J.; Zheng, W. *ACS Appl. Mater. Interfaces* **2011**, *3*, 3103−3109.
(19) Kao, S.-W.; Zhu, Y.-J.; Wu, J.; Wang, K.-W.; Tang, Q.-L. *Nanoscale Res. Lett.* **2010**, *5*, 781−785.
(20) Ko, F.-H.; Wu, C.-T. *Appl. Phys. Lett.* **2007**, *90*, 191901.
(21) Van Oss, C. J.; Chaudhury, M. K.; Good, R. *J. Chem. Rev.* **1988**, *88*, 927.
(22) Park, J.; Bae, J.-H.; Kim, W.-H.; Kim, M.-H.; Keum, C.-M.; Lee, S.-D.; Choi, J. S. *Materials* **2010**, *3*, 3614−3624.
(23) Kim, J.; Lim, S. H.; Kim, Y. S. *J. Am. Chem. Soc.* **2010**, *132*, 14721−14723.
(24) Noh, Y.-Y.; Sirringhaus, H. *Org. Electron.* **2009**, *10*, 174−180.
(25) Yoon, M.-H.; Yan, H.; Facchetti, A.; Marks, T. J. *J. Am. Chem. Soc.* **2005**, *127*, 10388−10395.
(26) Wu, Y. Q.; Lin, H. C.; Ye, P. D.; Wilk, G. D. *Appl. Phy. Lett.* **2007**, *90*, 072105.
(27) Liu, J.; Buchholz, D. B.; Hennek, J. W.; Chang, R. P. H.; Facchetti, A.; Marks, T. J. *J. Am. Chem. Soc.* **2010**, *132*, 11934−11942.
(28) Li, X.-C.; Sirringhaus, H.; Garnier, F.; Moratti, S. C.; Feeder, N.; Friend, R. H. *J. Am. Chem. Soc.* **1998**, *120*, 2206−2207.
(29) Kim, D. H.; Lee, D. Y.; Lee, H. S.; Lee, Y. H.; Kim, Y. H.; Han, J. I.; Cho, K. *Adv. Mater.* **2007**, *19*, 678−682.
(30) Kim, D. H.; Lee, H. S.; Yang, H.; Yang, L.; Cho, K. *Adv. Func. Mater.* **2008**, *18*, 1363−1370.
(31) Seol, Y. G.; Lee, J. G.; Lee, N.-E. *Org. Electron.* **2007**, *8*, 513−521.
(32) Djuric, T.; Ules, T.; Flesch, H.-G.; Plank, H.; Shen, Q.; Teichert, C.; Resel, R.; Ramsey, M. G. *Cryst. Growth Des.* **2011**, *11*, 1015−1020.
(33) Kaur, I.; Jia, W.; Kopreski, R. P.; Selvarasah, S.; Dokmeci, M. R.; Pramanik, C.; McGruer, N. E.; Miller, G. P. *J. Am. Chem. Soc.* **2008**, *130*, 16274−16286.
(34) Maliakal, A.; Raghavachari, K.; Katz, H.; Chandross, E.; Siegrist, T. *Chem. Mater.* **2004**, *16*, 4980−4986.
(35) Lu, Y.; Lee, W. H.; Lee, H. S.; Jang, Y.; Cho, K. *Appl. Phys. Lett.* **2009**, *94*, 113303.
(36) Roberts, M. E.; Queraltó, N.; Mannsfeld, S. C. B.; Reinecke, B. N.; Knoll, W.; Bao, Z. *Chem. Mater.* **2009**, *21*, 2292−2299.
(37) Yang, C.; Yoon, J.; Kim, S. H.; Hong, K.; Chung, D. S.; Heo, K.; Park, C. E.; Ree, M. *Appl. Phy. Lett.* **2008**, *92*, 243305.